Ketones were analyzed on column B, with butyrophenone as standard. Relative detector responses were determined for undeuterated samples; the responses of deuterated and undeuterated samples were assumed equal on a weight basis. In both cases, the yield of Grignard reagent, taken as equivalent to hydrocarbon produced by hydrolysis after replacement of the solvent, was about 90%. In all samples, reaction of the nitrile was complete before hydrolysis of the reaction mixture. The material balance after reaction with benzonitrile was approximately quantitative (100 ± 10%); uncertainties in the total solution volumes made a more accurate determination difficult. Three tubes were analyzed for each reaction, and three or more replicate GC analyses were made for each tube. Areas were calculated as peak height times width at half-height; relative areas agreed within ±1% with those from cutting and weighing peaks.

In each of the experiments, relative rate constants were determined by substitution into the integrated form of the equation for competition between two reactants for a single reagent[2] [$k_A/k_B = \ln (A_t/A_0)/\ln (B_t/B_0)$, where A_0 and B_0 are initial reactant concentrations and A_t and B_t are final concentrations]. If the yield is taken as quantitative, then the three pieces of data—initial concentration of Grignard reagent, final concentration of Grignard reagent, and concentration of product—provide a redundancy that allows three different combinations to be used in the calculation. Results are summarized in Table I.

Acknowledgment. We thank Mr. Frank Laib for assistance with mass spectrometric analyses and Jeffrey R. Schneider for help in the gas chromatographic measurements.

Registry No. 1, 110-53-2; 1-d_2, 77734-75-9; 1-bromohexane, 111-25-1; phenylacetylene, 536-74-3; benzonitrile, 100-47-0; deuterium, 7782-39-0; pentanoyl chloride, 638-29-9; 1-pentanol-*1,1*-d_2, 35658-10-7.

Preparation and Properties of Paramagnetic Bis(η-butadiene)(Lewis base)manganese Complexes[†]

R. L. Harlow, P. J. Krusic, R. J. McKinney, and S. S. Wreford*

Central Research and Development Department, Experimental Station, E. I. du Pont de Nemours and Company, Wilmington, Delaware 19898

Received April 12, 1982

$MnCl_2$ reacts with $Mg(C_4H_6)\cdot 2THF$ in the presence of Lewis bases and butadiene to form stable, monomeric Mn(0) complexes, $Mn(\eta\text{-}C_4H_6)_2L$ (L = PMe_3, PEt_3, $P(OMe)_3$ and CO). The related derivatives $Mn(\eta\text{-}2,3\text{-}Me_2C_4H_4)_2P(OMe)_3$ and $Mn(\eta\text{-}2\text{-}MeC_4H_5)_2PMe_3$ were prepared by cocondensation of substituted butadienes, $P(OMe)_3$ or PMe_3, and Mn atoms. The trimethyl phosphite and carbonyl adducts are rapidly reduced by Na/Hg, forming salts of the closed-shell anions $Mn(\eta\text{-}C_4H_6)_2L^-$; NBu_4^+ and $Na(18\text{-crown-}6)^+$ salts of $Mn(\eta\text{-}C_4H_6)_2P(OMe)_3^-$ were isolated. The Mn(0) compounds are 17-electron, fully paramagnetic complexes and show no propensity for dimerization. Crystals of $Mn(\eta\text{-}C_6H_6)_2P(OMe)_3$ are monoclinic, space group $P2_1/c$, with unit-cell dimensions at −100 °C of $a = 14.137$ (2), $b = 7.841$ (1), $c = 12.017$ (2) Å, and $\beta = 97.73$ (1)°. The refinement of 229 variables (all atomic coordinates, isotropic thermal parameters for H, anisotropic for Mn, P, O, and C) using 2245 reflections converged at $R = 0.037$ and $R_w = 0.032$. The Mn coordination can be described as a square pyramid with axial η^4-butadiene ligands and an apical $(CH_3O)_3P$ group. The butadiene ligands have Mn–C(internal) bond lengths that average 2.070 Å, Mn–C(terminal)'s that average 2.137 Å, and C–C bond lengths that are nearly equivalent and average 1.408 Å within a range of ±0.005 Å. ESR spectra with resolvable ^{55}Mn and ^{31}P hyperfine are observable in solution and frozen solution. Frozen solution spectra have highly anisotropic ^{55}Mn hyperfine components, one component being much larger than the other two. This observation is consistent with EHMO calculations that place the unpaired electron in an orbital oriented perpendicular to the C_2 axis and directed toward the butadiene ligands. These compounds do not undergo associative substitution reactions with facility. The EHMO calculations suggest that the deformations necessary to approach the transition state for such a displacement reaction are energetically unfavorable.

Recently, we reported that $Mg(C_4H_6)\cdot 2THF$ is a conveniently prepared, useful reagent for the preparation of transition-metal butadiene complexes.[1] The compound was found to react with a wide variety of transition-metal halides, affording the corresponding butadiene complexes with, generally, superior yields in comparison to more conventional procedures. While surveying the reactions of $Mg(C_4H_6)\cdot 2THF$, we found that it reacted with manganese chloride in the presence of lewis bases and excess butadiene to yield compounds with the stoichiometry $Mn(C_4H_6)_2$(Lewis base). These derivatives are formally analogous to $Mn(CO)_5$, a short-lived, 17-electron, organometallic radical with a controversial chemistry,[2] which has only very recently been definitively characterized by low-temperature matrix-isolation ESR[3] and IR[4] techniques. The determination of the chemical and physical properties of these manganese butadiene complexes appeared to be of value in order to assess the similarities and differences between these stable paramagnetic species and the $Mn(CO)_5$ radical, whose lifetime is essentially controlled by diffusion kinetics.[5] $Mn(\eta\text{-}C_4H_6)_2(CO)$ has been previously

---

[†] Contribution No. 3031.

[1] Wreford, S. S.; Whitney, J. F. *Inorg. Chem.* **1981**, *20*, 3918.

[2] (a) Byers, B. H.; Brown, T. L. *J. Am. Chem. Soc.* **1977**, *99*, 2527. (b) Kidd, D. R.; Brown, T. L. *Ibid.* **1978**, *100*, 4095. (c) Brown, T. L. *Ann. N.Y. Acad. Sci.* **1980**, *333*, 80. (d) Wrighton, M. S.; Ginley, D. S. *J. Am. Chem. Soc.* **1975**, *97*, 2065. (e) Poë, A. *Inorg. Chem.* **1981**, *20*, 4029 and 4032. (f) Atwood, J. D. *Ibid.* **1981**, *20*, 4031. (g) Fawcett, J. P.; Poë, A.; Sharma, K. R. *J. Chem. Soc., Dalton Trans.* **1979**, 1886. (h) Sweany, R. L.; Halpern, J. *J. Am. Chem. Soc.* **1977**, *99*, 8335. (i) Fox, A.; Malito, J.; Poë, A. *J. Chem. Soc., Chem. Commun.* **1981**, 1053.

[3] Howard, J. A.; Morton, J. R.; Preston, K. F. *Chem. Phys. Lett.* **1981**, *83*, 226.

[4] Church, S. P.; Poliakoff, M.; Timney, J. A.; Turner, J. J. *J. Am. Chem. Soc.* **1981**, *103*, 7515.

0276-7333/82/2301-1506$01.25/0

prepared and structurally characterized;[6] however, the complex and inefficient preparative method employed precluded syntheses on an appreciable scale. Little information was available about this compound beyond its X-ray crystal structure. Since multigram quantities of $Mn(C_4H_6)_2$ (Lewis base) are readily available by use of $Mg(C_4H_6)\cdot 2THF$, we have investigated the structural, chemical, and electronic properties of these compounds. The results of these studies and probable explanations for the similarities and differences of these derivatives to $Mn(CO)_5$ are reported below.

Experimental Section

All manipulations were performed under an atmosphere of prepurified nitrogen. Solvents were distilled from sodium benzophenone ketyl. Anhydrous $MnCl_2$ was purchased from Cerac; all phosphines were obtained from Strem Chemicals. $Mg(C_4H_6)\cdot 2THF$ was prepared by the literature method.[1,7] ESR spectra were obtained with a Bruker ER-420 instrument equipped with a field-tracking proton NMR gaussmeter (B-NM 12). A field-marking system and continuous measurement of the microwave frequency, both interacting with a BNC-12 computer, allowed the precise computer measurement of ESR splittings and *g* values. Elemental analyses and mass spectra were performed by the Central Research Analytical Division.

$Mn(\eta\text{-}C_4H_6)_2(PMe_3)$ (1). To a flask containing 2.83 g (22.5 mmol) of $MnCl_2$, 50 mL of THF, and 2.3 g (30.2 mmol) of PMe_3 was added, dropwise, a slurry of 15 g (22.5 mmol) of $Mg(C_4H_6)\cdot 2THF$ in 50 mL of THF. During the addition, the vessel was maintained at 0 °C, and butadiene was bubbled into the reaction mixture. The resulting green-brown solution was warmed to room temperature, stirred for 1 h, and then evaporated to dryness. The residue was extracted with 3 × 75 mL of boiling hexane. The pooled extracts were filtered, concentrated to 25 mL, and cooled to −20 °C overnight. The resulting green crystals of 1 were collected by filtration and dried in vacuo: 4.20 g (17.6 mmol, 78%); solution magnetic susceptibility (benzene)[8] $\mu_{eff}^{corr} = 1.74\ \mu_B$; mass spectrum, *m/e* 239.0775 (calcd 239.0761 for $^{12}C_{11}{}^{1}H_{21}{}^{55}Mn^{31}P$).

Anal. Calcd for $C_{11}H_{21}MnP$: C, 55.23; H, 8.85. Found: C, 54.48; H, 8.84.

$Mn(\eta\text{-}C_4H_6)_2(PEt_3)$ (2). In a similar manner, 1.33 g of $MnCl_2$, 4.70 g of $Mg(C_4H_6)\cdot 2THF$, and 5.0 mL of PEt_3 were reacted. Green crystals of 2 were isolated by recrystallization from hexane (0.63 g, 21%): solution magnetic susceptibility (benzene)[8] $\mu_{eff}^{corr} = 1.60\ \mu_B$; mass spectrum, *m/e* 281.1273 (calcd for $^{12}C_{14}{}^{1}H_{27}{}^{55}Mn^{31}P$ 281.1231).

Anal. Calcd for $C_{14}H_{27}MnP$: C, 59.78; H, 9.68. Found: C, 57.37; H, 9.56.

$Mn(\eta\text{-}C_4H_6)_2P(OMe)_3$ (3) from $Mg(C_4H_6)\cdot 2THF$. Similarly, 2.83 g of $MnCl_2$, 3.0 g of $P(OMe)_3$, and 5.0 g of $Mg(C_4H_6)\cdot 2THF$ were reacted. After recrystallization from hexane, 0.90 g (14%) of green, crystalline 3 were isolated: solution magnetic moment (benzene)[8] $\mu_{eff}^{corr} = 1.63\ \mu_B$; mass spectrum, *m/e* 287.0629 (calcd for $^{12}C_{11}{}^{1}H_{21}{}^{55}Mn^{16}O_3{}^{31}P$ 287.0579), 233.0158 (calcd for $M^+ - C_4H_6$ 233.0109).

Anal. Calcd for $C_{11}H_{21}MnO_3P$: C, 46.00; H, 7.37. Found: C, 45.34; H, 7.48.

$Mn(\eta\text{-}C_4H_6)_2(CO)$ (4). Similarly, 2.83 g of $MnCl_2$ and 5.0 g of $Mg(C_4H_6)\cdot 2THF$ were reacted in the presence of excess butadiene while CO was bubbled through the solution. After evaporation of the solvent, the dark brown residue was exposed to the atmosphere for 2–3 min. The solid warmed and turned green. Workup in hexane as described above afforded 0.14 g (3.3%) of 4, identified by comparison of its IR and mass spectrum with the literature report.[6a]

$Mn(\eta\text{-}C_4H_6)_2P(OMe)_3$ (3) from Mn Atoms. A Planar metal atom evaporation device was fitted for resistive heating and charged with Mn metal. While the Mn (380 W) was evaporated onto the walls of a liquid-nitrogen-cooled reaction vessel, a mixture of 60 mL of butadienes (−78 °C) in 60 mL of $P(OMe)_3$ was vaporized and sprayed into the apparatus at the rate of 1–2 mL/min. After the addition was complete, the apparatus was warmed to room temperature and the contents were rinsed into a flask with the aid of 100 mL of THF. The mixture was evaporated to dryness and the residue extracted with boiling hexane. The pooled extracts were filtered through an alumina pad and concentrated. Cooling afforded 1.1 g of 3 (2.5% based on 10.4 g Mn evaporated).

$Mn[\eta\text{-}2,3\text{-}(CH_3)_2C_4H_4]_2PMe_3$ (5). A Planar metal atom evaporation apparatus was fitted for resistive heating and charged with 12.1 g of Mn (0.22 mol). A mixture of 25 g of PMe_3 (0.33 mol) and 54 g of 2,3-dimethylbutadiene (0.66 mol) was admitted to the liquid-nitrogen-cooled reaction flask at the rate of 1 mL/min while the Mn (480 W) was evaporated. When the addition was complete, the vessel was warmed to room temperature, and the contents were rinsed into a flask with the aid of 50 mL of THF. The green-brown solution was filtered and evaporated to dryness. The resulting dark residue was extracted with 75 mL of boiling hexane; the extract was filtered and concentrated. Cooling afforded 2.36 g (4%) of green, crystalline 5: solution magnetic susceptibility (benzene)[8] $\mu_{eff}^{corr} = 1.70\ \mu_B$; mass spectrum, *m/e* 295.1391 (calcd for $^{12}C_{15}{}^{1}H_{29}{}^{31}P^{55}Mn$ 295.1387).

Anal. Calcd for $C_{15}H_{29}PMn$: C, 60.85; H, 10.14. Found: C, 60.94; H, 9.98.

$Mn(\eta\text{-}2\text{-}CH_3C_4H_5)_2[P(OMe)_3]$ (6). With use of an analogous procedure, 13.38 g of Mn (0.24 mol), 68 g of isoprene (1.0 mol), and 62 g of $P(OMe)_3$ (0.5 mol) were reacted. The reaction mixture was rinsed from the vessel with 100 mL of THF and evaporated to dryness. After the resulting residue was extracted with 3 × 100 mL of boiling hexane, the pooled extracts were filtered through a 1-in. pad of alumina. The eluent was evaporated to dryness, affording a deep green oil which could not be induced to crystallize. The compound was identified as 6 on the basis of its high-resolution mass spectrum, *m/e* 315.0947 (calcd for $^{12}C_{13}{}^{1}H_{25}{}^{55}Mn^{16}O_3{}^{31}P$ 315.0923).

$[N(C_4H_9)_4][Mn(\eta\text{-}C_4H_6)_2P(OMe)_3]$ (7). A solution of 1.07 g of 3 (3.8 mmol) in 50 mL of THF was stirred with 100 g of 1% Na/Hg. A red solution formed immediately. After being stirred 2 h, the solution was decanted, filtered, and treated with 1.3 g of tetrabutylammonium perchlorate. After being stirred 10 min, the solution was filtered and evaporated to a thick oil which solidified on cooling in the presence of ether overnight. The resulting 2.11 g of crude, red 7 was collected by filtration and dried in vacuo. Red needles of pure 7 could be obtained by recrystallization from Et_2O–THF.

Anal. Calcd for $C_{27}H_{57}MnNO_3P$: C, 61.23; H, 10.85. Found: C, 59.58; H_2, 10.70.

[Na(1,4,7,10,13,16-hexaoxacyclooctadecane)][$Mn(\eta\text{-}C_4H_6)_2P(OMe)_3$] (8). A solution of 1.0 g of 3 (4.3 mmol) in 15 mL of THF was stirred with 100 g of 1% Na/Hg. After 30 min, the resulting red solution was decanted and evaporated to dryness. The red solid residue was washed with Et_2O and treated with 0.92 g of 18-crown-6 (3.5 mmol) in 15 mL of THF. The purple-red solution was evaporated to dryness, and the crude product was recrystallized THF–Et_2O; 0.89 g of crystalline, red 8 (36%) was obtained.

Anal. Calcd for $C_{23}H_{45}MnNaO_9P$: C, 48.09; H, 7.90; Mn, 9.56; P, 5.39. Found: C, 47.77; H, 7.94; Mn, 9.68; P, 5.17.

Crystal Structure of 3. The crystal selected for the X-ray diffraction study was a thin plate measuring 0.07 × 0.30 × 0.31 mm. It was sealed in a glass capillary and mounted on a Syntex P3 diffractometer (graphite monochromator, Mo Kα radiation, $\lambda = 0.71069$ Å) where it was cooled to −100 °C. Unit cell dimensions were refined from the Bragg angles of 50 reflections in the range $24 < 2\theta < 26°$: $a = 14.137$ (2) Å, $b = 7.841$ (1) Å, $c = 12.017$ (2) Å, $\beta = 97.73$ (1)°. The cell volume, 1322 Å^3, yields a calculated density of 1.443 g cm^{-3} for $Z = 4$. The systematic absences were consistent with the monoclinic space group $P2_1/c$.

Intensity data for 3039 reflections were collected by using the ω scan techniques ($4 < 2\theta < 55°$; scan width of 1.0°; background

---

(5) (a) Hughey, J. L. IV; Anderson, C. P.; Meyer, T. J.: *J. Organomet. Chem.* **1977**, *125*, C49. (b) Waltz, W. L.; Hackelberg, O.; Dorfman, L. M.; Wojcicki, A. *J. Am. Chem. Soc.* **1978**, *100*, 7259. (c) Wegman, R. W.; Olsen, R. J.; Gard, D. R.; Faulkner, L. R.; Brown, T. L. *Ibid.* **1981**, *103*, 6089.

(6) (a) Heberhold, M.; Razavi, A. *Angew. Chem.* **1975**, *87*, 351. (b) Huttner, G.; Neugebauer, D.; Razavi, A. *Ibid.* **1975**, *87*, 353.

(7) (a) Fujita, K.; Ohnuma, Y.; Yasuda, H.; Tani, H. *J. Organomet. Chem.* **1976**, *113*, 201. (b) Yasuda, H.; Nakano, Y.; Natsukawa, K.; Tani, H. *Macromolecules* **1978**, *11*, 586.

(8) Evans, D. F. *J. Chem. Soc.* **1959**, 2003.

(9) Nugent, W. A.; Harlow, R. L. *Inorg. Chem.* **1979**, *18*, 2030.

Table I. Selected Bond Distances (Å) and Bond Angles (Deg) with Estimated Standard Deviations

Bond Distances

Mn-P	2.188 (1)	Mn-C(3)	2.072 (2)	Mn-C(6)	2.073 (2)
Mn-C(1)	2.137 (3)	Mn-C(4)	2.141 (3)	Mn-C(7)	2.065 (2)
Mn-C(2)	2.068 (3)	Mn-C(5)	2.141 (2)	Mn-C(8)	2.129 (2)
P-O(1)	1.616 (2)	P-O(2)	1.617 (2)	P-O(3)	1.609 (2)
O(1)-C(11)	1.430 (3)	O(2)-C(12)	1.436 (3)	O(3)-C(13)	1.447 (3)
C(1)-C(2)	1.404 (4)	C(2)-C(3)	1.405 (4)	C(3)-C(4)	1.407 (4)
C(5)-C(6)	1.414 (3)	C(6)-C(7)	1.408 (3)	C(7)-C(8)	1.409 (4)
C(1)-H(1)A	0.92 (3)	C(2)-H(2)	0.90 (3)	C(4)-H(4)A	0.97 (3)
C(1)-H(1)B	0.96 (3)	C(3)-H(3)	0.98 (2)	C(4)-H(4)B	0.91 (3)
C(5)-H(5)A	0.92 (3)	C(6)-H(6)	0.95 (2)	C(8)-H(8)A	0.91 (3)
C(5)-H(5)B	0.97 (2)	C(7)-H(7)	0.94 (3)	C(8)-H(8)B	0.96 (2)

Bond Angles

Mn-P-O(1)	121.46 (7)	Mn-P-O(3)	113.73 (7)	O(1)-P-O(3)	103.1 (1)
Mn-P-O(2)	121.40 (7)	O(1)-P-O(2)	91.0 (1)	O(2)-P-O(3)	102.2 (1)
P-O(1)-C(11)	119.1 (2)	P-O(2)-C(12)	117.6 (2)	P-O(3)-C(13)	121.1 (2)
C(1)-C(2)-C(3)	119.6 (3)	C(5)-C(6)-C(7)	118.9 (2)	C(6)-C(7)-C(8)	119.5 (2)
C(2)-C(3)-C(4)	118.8 (3)				

measurements at both ends of the scan; total background time equal to scan time). The intensities of four standard reflections were monitored periodically and showed only statistical variations (less than ±1.6σ(*I*)). An absorption correction was made by using the ψ-scan technique; transmission factors ranged from 0.847 to 0.999.

The structure was solved by direct methods; the positions of the hydrogen atoms were calculated. Full-matrix least-squares refinement of all positional and thermal parameters (anisotropic for Mn, P, O, and C; isotropic for H) with 2245 reflections with $I > 2\sigma(I)$ converged at $R = 0.037$ and $R_w = 0.032$. All peaks in the final difference Fourier were less than 0.22 e Å^{-3} with the largest peaks near the Mn and P atoms. The mathematical and computational details may be found elsewhere.[9]

Selected bond lengths and angles are in Table I. Coordinates for non-hydrogen atoms are in Table IV. Coordinates for hydrogen atoms (Table V), thermal parameters (Table VI), least-squares planes (Table VII), and structure factor amplitudes (Table VIII) are available as supplementary material.

Results and Discussion

Preparation of Complexes. Treatment of anhydrous $MnCl_2$ with magnesium butadiene in the presence of excess butadiene and a Lewis base afforded the paramagnetic, 17-electron derivatives shown in eq 1. Excellent yields

$$MnCl_2 + Mg(C_4H_6)\cdot 2THF + C_4H_6 + L \rightarrow MgCl_2 + Mn(C_4H_6)_2L \quad (1)$$

1, L = PMe_3
2, L = PEt_3
3, L = $P(OMe)_3$
4, L = CO

were obtained when alkylphosphines with a small cone angle were used. However, no analogous products could be isolated when reactions were attempted with triphenyl- or triisopropylphosphine. A green oil was formed for L = PMe_2Ph, but the material could not be crystallized and further purification was not effected. Use of trimethyl phosphite or carbon monoxide resulted in very poor yields of **3** and **4**, respectively. Indeed, **4** could not be detected in the reaction mixture until it had been treated with small amounts of air. Presumably, **3** and **4**, being readily reduced to the corresponding anions (vide infra), are reduced by the magnesium butadiene reagent at a rate competitive with their initial formation. At least in the case of **4**, small amounts of the neutral complex were formed by subsequent air oxidation of the presumed reduction product, $[Mn(C_4H_6)_2(CO)]^-$. The high yields of **1** and **2** are consistent with this interpretation as the alkylphosphine derivatives were found to be resistant to reduction.

The complex **4** has been prepared previously by photolysis of $Mn(CO)_4NO$ in the presence of butadiene and isolated in 4% yield after a complex chromatographic workup (eq 2).[6a] The procedure based on eq 1 is more

$$Mn(CO)_4NO + C_4H_6 \xrightarrow[h\nu]{} Mn(C_4H_6)(CO)_2NO + 4 \quad (2)$$

convenient and more easily scaled up. At least for the phosphine adducts **1**–**3**, 5-g quantities of the derivatives can be readily prepared.

The metal atom evaporation technique was found to be a useful synthetic method for preparation of $Mn(\eta\text{-}C_4H_6)_2L$ complexes, particularly for derivatives containing substituted butadiene ligands. Magnesium reagents analogous to $Mg(C_4H_6)\cdot 2THF$ with substituted butadienes have been prepared and react similarly but are difficult to purify.[7b] The metal atom technique, although it affords low yields, is more convenient in these cases. Isoprene and 2,3-dimethylbutadiene derivatives were prepared by this method as shown in eq 3.

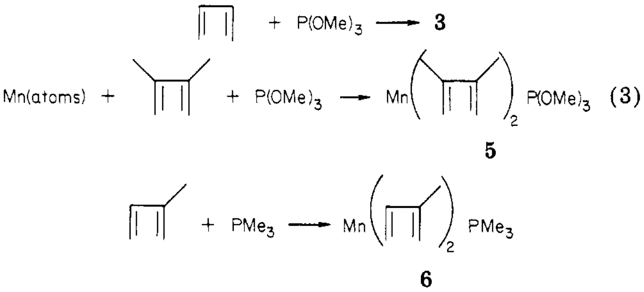

(3)

Properties of Complexes. All available physical evidence is consistent with monomeric formulations for compounds **1**–**6**. Solution magnetic moments of ~1.7 μ_B were measured by the Evan's method[8] for **1**–**3** and **5**. All the complexes had mass spectra consistent with monomeric formulations. ESR spectra (vide infra) were observed for **1**, **2**, and **4** with hyperfine splittings requiring monomeric MnP and Mn(CO) fragments, respectively. X-ray structures of **4** and **3** show a monomeric molecular unit in the solid state.

The compounds **1** and **3** have similar electronic spectra. THF solutions have two weak absorbances (λ_{max} = 747 and 588 nm for **1** and 722 and 600 nm for **3**) with extinction coefficients of ca. 50 and two shoulders in the ultraviolet region (λ_{max} = 420 and 320 nm for **1** and **3**). In both cases, Beer's law is followed over the range 10^{-2}–10^{-4} M as expected for monomeric compounds.

Stirring THF solutions of **3** or **4** with sodium amalgam resulted in rapid formation of a red solution containing the 18-electron anions $Mn(\eta\text{-}C_4H_6)_2L^-$, analogous to $Mn(CO)_5^-$.

$$Mn(C_4H_6)_2P(OMe)_3 + Na/Hg \rightarrow Mn(C_4H_6)_2P(OMe)_3^-$$

$$Mn(C_4H_6)_2(CO) + Na/Hg \rightarrow Mn(C_4H_6)_2(CO)^- \quad (4)$$

Tetrabutylammonium and Na(18-crown-6) salts of $Mn(C_4H_6)_2P(OMe)_3^-$ were isolated by metathetical procedures or by treatment with the crown ether, respectively. Brief exposure of solutions of these anions to air regenerated the neutral, paramagnetic precursors. In contrast to the known chemistry of $Mn(CO)_5^-$,[10] treatment of solutions of $Mn(C_4H_6)_2P(OMe)_3^-$ with methyl iodide or $HBF_4{\cdot}Et_2O$ did not afford stable alkyl or hydride derivatives; in both cases, the anion was oxidized and **3** was recovered. Alkylphosphine adducts were not reduced analogously to **3** and **4**. Stirring **1** with Na/Hg for 24 h did not result in its conversion to reduced products; **1** could be recovered unchanged after treatment with Na/Hg.

The complex **1** did not react with 1 atm of hydrogen and was not oxidized by excess benzyl bromide at room temperature. However, all the complexes **1–6** were rapidly oxidized by air, forming MnO_2. Treatment of **1** with $AgBF_4$ in THF led to formation of silver metal and red-brown solutions. No tractable cationic products could be isolated, however, even when the oxidation was conducted in the presence of excess PMe_3.

Although $Mn(CO)_5$ radicals are thought to be intermediates in substitution reactions of $Mn_2(CO)_{10}$ and are generally considered to be very substitutionally labile,[2] complexes **1–6** appear to be substitutionally quite inert. Also, they undergo slow ligand substitution reactions, which were monitored by ESR (vide infra), only under UV irradiation.

ESR Results. The ESR and IR spectra of the reactive $Mn(CO)_5$ radical have been sought by many investigators for a long time. A definitive spectroscopic characterization of this species, however, was not available until very recently. In a matrix isolation IR study,[4] $Mn(CO)_5$ was prepared by UV photolysis of $HMn(CO)_5$ in solid CO matrices at 10–20 K. ^{13}C isotopic labeling studies showed that it has a square pyramidal, C_{4v}, structure with an axial–equatorial bond angle of 96 ± 3°. This is the structure predicted by various molecular orbital calculations[11-14] which place the unpaired electron in a highly directional a_1 orbital, with large $3d_{z^2}$ character, pointing along the axis of the pyramid and toward the empty ligand site. The radical is thus ideally set up for rapid dimerization or recombination with another radical. In an ESR study,[3] $Mn(CO)_5$ was prepared by reaction between Na or Ag atoms and $Mn(CO)_5Cl$ or $Mn(CO)_5Br$ on a rotating cryostat at 77 K using perdeuteriobenzene as a diluent and inert matrix. The species was found to have axially symmetric **g** and ^{55}Mn hyperfine **A** tensors with the following components: $g_\parallel = 2.000 \pm 0.003$; $g_\perp = 2.038 \pm 0.003$; $A_\parallel = 66 \pm 3$ G; $A_\perp = 30 \pm 3$ G. A comparison with the isoelectronic $Fe(CO)_5^+$ radical cation species[15] indicated that the parallel and perpendicular components of the **A** tensor are most probably of opposite sign (66, −30, −30 G). It was estimated that these parameters correspond to 51% $3d_{z^2}$ character for the a_1 orbital containing the unpaired electron. The above sign choice predicts that the isotropic Mn coupling constant for $Mn(CO)_5$ should be quite small ($A_{iso} = {}^1/_3(A_\parallel + 2A_\perp) = 2$ G) and, therefore, that the solution ESR spectrum of the $Mn(CO)_5$ radical, when detected, will probably consist of a single broad line.

Table II. ESR Parameters of $Mn(\eta\text{-}C_4H_6)L$ in Toluene at Room Temperature

L	g_{iso}	a_{iso}(Mn), G	a_{iso}(P), G
CO (**4**)	2.0131	83.6	
$P(OMe)_3$ (**3**)	2.0163	83.2	28.6
PMe_3 (**1**)	2.0182	82.6	26.7

The ESR parameters for $Mn(CO)_5$ are quite consistent with the parameters for the related species $Mn(CO)_3(PBu_3)_2$ which were reported earlier.[16] In contrast to $Mn(CO)_5$, the phosphine-substituted analogue is sufficiently stable so that its dilute heptane solutions could be studied in the solid as well as in the liquid state. At 83 K, the ^{55}Mn **A** tensor was found to be axially symmetric with components $A_\parallel = 54.1$ G and $A_\perp = 35.7$ G. The solution spectrum at room temperature, with an isotropic Mn coupling of only about 7 G, leaves no doubt about opposite signs for $A_\parallel$ and $A_\perp$, further supporting the same choice for $Mn(CO)_5$ which was based only on isoelectronic arguments.[3] The phosphorus splitting is quite isotropic, having a value of 20 ± 1 G both in solution as well as in the solid state. It was concluded that this spectrum is consistent with $Mn(CO)_3(PBu_3)_2$ having an idealized square-pyramidal geometry with the phosphines occupying mutually trans basal positions. Thus, $Mn(CO)_5$ and $Mn(CO)_3(PBu_3)_2$ are electronically and spectroscopically quite similar. The very slow dimerization of the latter compared to the essentially diffusion-controlled dimerization of the former was attributed not to differences in electronic structure but to the steric requirements of the phosphine ligands in basal positions. It was argued that the monomer must first rearrange to a less stable configuration with one phosphine in the axial position before dimerizing. The stereochemistry of the related $Mn_2(CO)_8L_2$ dimers, with the L ligands invariably in axial positions, was thought to support this view.

Although the complexes of this report, $Mn(\eta\text{-}C_4H_6)_2L$, are ostensibly analogous to the $Mn(CO)_5$ and $Mn(CO)_3(PBu_3)_2$ species discussed above, the ESR data detailed below reveal that this analogy is misleading and that these species are, in fact, electronically quite different, in agreement with molecular orbital considerations (vide infra).

Dilute solutions ($<10^{-3}$ M) of $Mn(\eta\text{-}C_4H_6)_2L$ in toluene give intense ESR spectra with a characteristic six-line splitting as the result of a hyperfine interaction with a single ^{55}Mn ($I = {}^5/_2$) nucleus. In the presence of a phosphine ligand, each line is further split into a doublet by a weaker interaction with one ^{31}P ($I = {}^1/_2$) nucleus. No hyperfine structure for the protons of the butadiene ligands could be resolved. The intensities of the spectra were essentially temperature independent, indicating the absence of noticeable dimerization. The solution ESR parameters of **1**, **3**, and **4** are shown in Table II. Because of the large magnitude of the Mn isotropic coupling constant, the six lines of the ^{55}Mn hyperfine splitting pattern

---

[10] King, R. B. *Acc. Chem. Res.* **1970**, *3*, 417.

[11] Burdett, J. K. *J. Chem. Soc., Faraday Trans. 2* **1974**, *70*, 1599.

[12] Elian, M.; Hoffman, R. *Inorg. Chem.* **1975**, *14*, 1058.

[13] Demuynck, J.; Strich, A.; Veillard, A. *Nouv. J. Chim.* **1977**, *1*, 217.

[14] Pensak, D. A.; McKinney, R. J. *Inorg. Chem.* **1979**, *18*, 3407.

[15] Lionel, T.; Morton, J. R.; Preston, K. F. *J. Chem. Phys.* **1982**, *76*, 234.

[16] Kidd, D. R.; Cheng, C. P.; Brown, T. L. *J. Am. Chem. Soc.* **1978**, *100*, 4103.

Table III. ESR Parameters of $Mn(\eta\text{-}C_4H_6)_2L$ in 3-Methylpentane[a]

	L			
	CO	$P(CH_3)_3$	$Mn(CO)_5$[b]	$Mn(CO)_3$-$(PBu_3)_2$[d]
g_1	1.992	1.991	2.000	2.040
g_2	2.0475	2.0511	2.038	2.040
g_3	2.023	2.022	2.038	2.040
A_1(Mn), G	163.5	163.6	66	54.1
A_2(Mn), G	<5	<5	−30	−35.7
A_3(Mn), G	73	68	−30	−35.7
A_1(P), G		28.2		20
A_2(P), G		29.2		19
A_3(P), G		27.8		19
g_{iso}	2.0137	2.0182	(2.025)[c]	2.030
a_{iso}(Mn), G	83.5	82.5	(2)[c]	7
a_{iso}(P), G		27.3		21

[a] Anisotropic parameters measured at −170 °C and isotropic parameters at −80 °C. [b] From ref 3. [c] Calculated from solid-state data. [d] From ref 16.

Table IV. Atomic Coordinates

atom	x	y	z
Mn	0.32435 (3)	0.43646 (5)	0.13625 (3)
P	0.18415 (5)	0.41143 (9)	0.19216 (5)
O(1)	0.1321 (1)	0.2284 (2)	0.1952 (2)
O(2)	0.1689 (1)	0.4486 (2)	0.3209 (1)
O(3)	0.1033 (1)	0.5291 (3)	0.1234 (1)
C(1)	0.3423 (2)	0.1660 (4)	0.1326 (3)
C(2)	0.4297 (2)	0.2529 (4)	0.1402 (3)
C(3)	0.4540 (2)	0.3708 (4)	0.2274 (3)
C(4)	0.3899 (2)	0.3979 (4)	0.3055 (2)
C(5)	0.2571 (2)	0.4721 (3)	−0.0327 (2)

are not equidistant. Therefore, the ^{55}Mn coupling constants were extracted to second order by using the expression

$$H(M) = H_0 - aM - a^2/2H_0[I(I+1) - M^2] \quad (5)$$

with $-5/2 \leq M \leq 5/2$ where $H(M)$ is the field of the Mth hyperfine component and H_0 is the center field. The g values were also calculated to second order by using the center fields H_0 calculated from the above expression by simple iterative procedures. The large values for the isotropic ^{55}Mn coupling of about 83 G for these complexes (Table II) is clearly in contrast to the small value expected for $Mn(CO)_5$ in solution and actually observed for the phosphine-disubstituted analogues.

The anisotropic ESR parameters of $Mn(\eta\text{-}C_4H_6)_2CO$ and $Mn(\eta\text{-}C_4H_6)_2PMe_3$ were extracted from the powder spectra obtained with dilute 3-methylpentane solutions frozen as clear glasses at −170 °C. The spectra at −80 and at −170 °C are shown in Figure 1, and the corresponding ESR parameters appear in Table III. A set of six absorptions corresponding to one of the **g** tensor components is immediately apparent in the powder spectrum of the CO derivative; five of these are labeled with triangles in Figure 1B while the sixth is obscured by another feature of the spectrum. The ^{55}Mn coupling extracted by using eq 5 from this group of lines has the very large value of 163.5 G. Closer scrutiny reveals that each of these absorptions has an additional hyperfine structure (see inset in Figure 1) caused by the protons of the butadiene ligands. The number of interacting protons must be even and greater than four since the structure is at least a binominal quintet of about 3-G splitting. For the PMe_3 derivative these six absorptions (A_1(Mn) = 163.6 G) are doubled by a weaker interaction with a phosphorus nucleus (A_1(P) = 28.2 G).

The remaining features of each powder spectrum could be interpreted as constituting a set of six perpendicular ^{55}Mn hyperfine components. Five of these are marked with circles in Figure 1B, and the sixth would be the truncated central line. The **A** and **g** tensors would then be axially symmetric. There is a problem with this interpretation, however, since the measured ^{55}Mn perpendicular coupling of 73 G for 4 and 68 G for 1 (these couplings cannot be measured as precisely as the others) cannot be reconciled with the observed solution Mn splittings. Thus, with the assumption of equal signs, the calculated isotropic value of 4 will be $a_{iso}(Mn) = {}^1/_3(A_{\parallel} + 2A_{\perp}) = 103$ G while with opposite signs $a_{iso}(Mn) = 6$ G, neither of which is close to the solution value of 83.5 G. The alternative is to assume three different components for each tensor, consistent with the C_{2v} symmetriy of the molecular structures (vide infra). The circled absorptions in Figure 1B would represent the Mn splitting along a second molecular axis, while the central truncated line would correspond to a third axis along which the Mn splitting is so small that it cannot be resolved. This would also explain the pronounced intensity of the central line. With the assumption that this small splitting is about 5 G and that all ^{55}Mn **A** tensor components are of *the same sign*, the calculated value of the isotropic ^{55}Mn splitting is $a_{iso} = {}^1/_3(A_1 + A2 + A_3) = 81$ G in excellent agreement with the observed solution splitting of 83.5 G for 4.

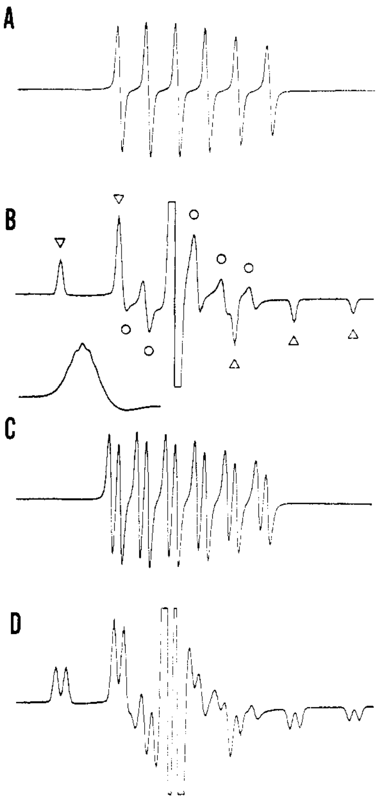

Figure 1. ESR spectra of $Mn(\eta\text{-}C_4H_6)_2CO$ in 3-methylpentane at (A) −80 °C and (B) −170 °C and of $Mn(\eta\text{-}C_4H_6)_2PMe_3$ at (C) −80 °C and (D) −170 °C. The inset shows an expansion of the second absorption from the left in B.

Computer simulation of the powder spectrum for Mn(butadiene)$_2$CO using the parameters of Table III confirms the correctness of the interpretation based on three different principal values for the **g** and **A** tensors. An improved match, shown in Figure 2, was obtained with A_2(Mn) = 1 G and by changing the value of g_2 to 2.03. An equally good match would have been obtained by keeping the g_2 value of Table III and altering appropriately the values of g_1 and g_3. We believe that the latter procedure would be physically more meaningful, although more laborious, since g_1 and g_3 are derived quantities, whereas g_2 was measured directly from the crossover point of the

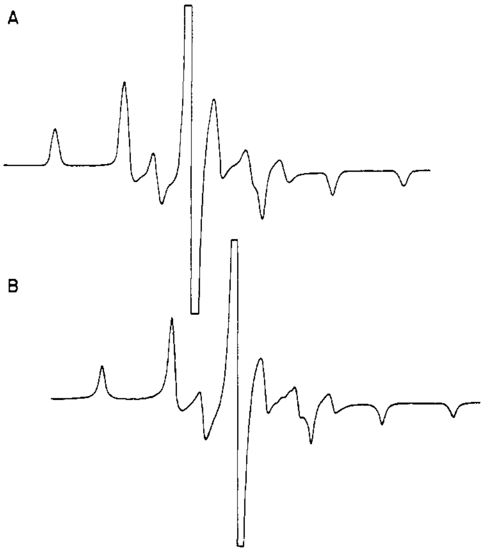

Figure 2. Experimental (A) and calculated (B) powder spectra of Mn(butadiene)$_2$CO.

sharp central line of the powder spectrum.

For the PMe$_3$ derivative, all spectral features of the powder spectrum show an additional doubling (Figure 1D) attributable to a hyperfine interaction with the phosphorus nucleus. It is seen in Table III that this interaction is quite isotropic, having the relatively small value of 28.5 ± 1 G along each of three principal molecular axes.

The ESR parameters for the Mn(butadiene)$_2$L species are compared with those for Mn(CO)$_5$ in Table III. Although the two types of complexes have a similar geometry best represented by a tetragonal pyramid (vide infra), the molecular orbitals containing the unpaired electron are of a quite different nature. This is most apparent in the ^{55}Mn **A** tensor that has two large components of the same sign for the butadiene complexes compared to opposite signs for $A_\parallel$ and $A_\perp$ in Mn(CO)$_5$. This leads to a large solution Mn splitting for the former in contrast to the very small solution splitting expected for the latter and actually observed for the Mn(CO)$_3$L$_2$ analogues. It is further evident that the direction corresponding to the maximum ^{55}Mn splitting in the butadiene complexes cannot be the axis of the tetragonal pyramid as it is for Mn(CO)$_5$. If this were the case, we would expect for 1 a highly anisotropic phosphorus hyperfine tensor with a large component along this axis. The proton interaction observed along the direction of maximum ^{55}Mn coupling suggests instead that this direction may be pointing toward the butadiene ligands, consistent with the molecular orbital considerations presented below.

The different electronic nature of the two types of 17-electron complexes is also apparent in their totally different substitutional behavior. Mn(CO)$_5$ is extraordinarily substitutionally labile and can exchange a CO ligand for a phosphine ligand within its very short lifetime, which is determined essentially by diffusion.[2] By contrast, no phosphine substitution is evident by ESR in 24 h at room temperature in a dilute pentane solution (10^{-3} M) of Mn(butadiene)$_2$CO to which a large excess of PMe$_3$ was added. Interestingly, this substitution can be forced in the same sample under the influence of UV irradiation provided by a low-pressure, mercury discharge coil enveloping the ESR sample tube. The spectra of Figure 3 were obtained for the starting solution and for the solution after successive 2-min periods of UV irradiation at room temperature. Within a total of 6 min of UV irradiation, the Mn(butadiene)$_2$CO is converted completely to Mn(butadiene)$_2$PMe$_3$. The forcing conditions required clearly indicate a very low efficiency for photosubstitution. It is thus incorrect to attribute substitutional lability to all 17-electron transition-metal carbonyl complexes.

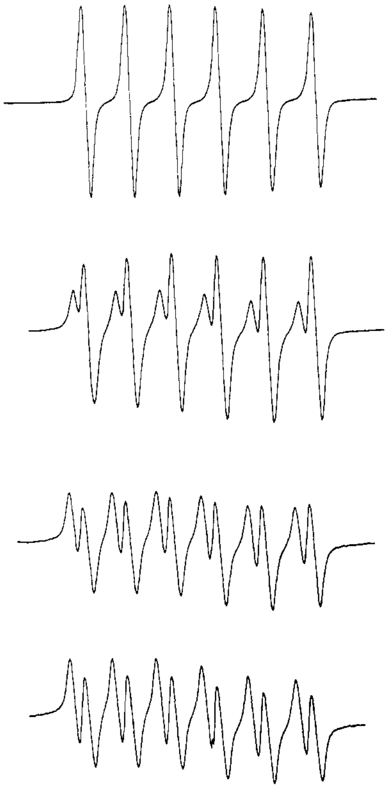

Figure 3. ESR spectra at room temperature of 10^{-3} M Mn(η-C$_4$H$_6$)$_2$CO in pentane in the presence of a large excess of PMe$_3$ (A) before UV irradiation, (B) after 2-min irradiation, (C) after 4-min irradiation, and (D) after 6-min irradiation.

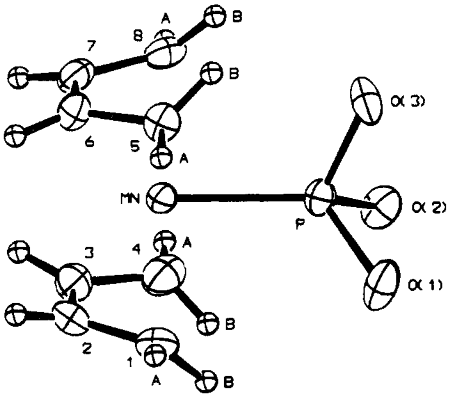

Figure 4. Molecular structure of Mn(η-C$_4$H$_6$)$_2$P(OMe)$_3$. Methyl groups omitted for clarity.

Structure of Mn(η-C$_4$H$_6$)$_2$P(OMe)$_3$. The structure of 3 is shown in Figure 4; it is based on a square-pyramidal arrangement with axial η^4-butadiene ligands and an apical trimethyl phosphite unit. The molecular symmetry is C_{2v}. The butadiene ligands are planar, and all C–C bond lengths are essentially equal. The methylene hydrogen atoms do not lie in the plane; syn and anti hydrogens are displaced ca. 0.5 Å away from and ca. 0.15 Å toward Mn, respectively. The methine hydrogens are similarly displaced ca. 0.15 Å toward Mn. The Mn–carbon distances follow the normal pattern for η^4-butadiene complexes;[17]

---

[17] Cotton, F. A.; Day, V.; Frenz, B. A.; Hardcastle, K. I.; Troup, J. M. *J. Am. Chem. Soc.* **1973**, *95*, 4522.

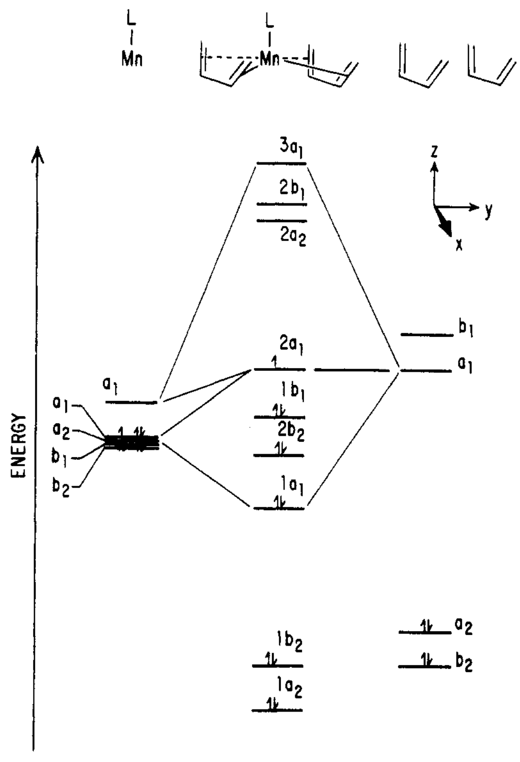

Figure 5. Orbital interaction diagram for Mn–L with two C_4H_6 groups.

i.e., the Mn–internal carbon (e.g., Mn–C_2) distances are shorter than the Mn–terminal carbon distances (e.g., Mn–C_1) by ca. 0.07 Å.

The structure is very similar to that found for 4.[6b] Some differences, which are likely derived from the different character of the axial ligands, are apparent in the butadiene ligands. Although the Mn–carbon distances are nearly equal for both compounds, the C–C bond distances differ substantially. For 3 one finds C(internal)–C(internal) has been shortened relative to 4 (1.406 vs. 1.46 Å) and C(internal)–C(terminal) has been lengthened (1.408 vs. 1.39 Å). This is a probable consequence of increased back-donation into the butadiene LUMO by Mn, a reflection of the increased electron density on Mn in 3 brought about by substitution of $P(OMe)_3$ for CO.

The unpaired electron in 3 or 4[6a] does not appear to occupy a stereochemical site or have a significant structural role.

The Electronic Structure of Mn(η-C_4H_6)$_2$L Derivatives. The thermal stability of 1–6 contrasts with the instability of the formally analogous 17-electron complex $Mn(CO)_5$ both in the tendency to dimerize as well as its substitutional lability. A semiempirical molecular orbital treatment[18] was carried out in order to gain insight into these differences.

An orbital interaction diagram for Mn–L with two butadiene (C_4H_6) groups is illustrated in Figure 5. The lowest energy π orbitals of the butadiene groups are not included because they are of such low energy as to have little interaction with the manganese d orbitals of interest to us (though they do count toward the 17-electron count). The strongest interactions are between the occupied a_2 and the unoccupied a_1 and b_1 orbitals of the butadienes and their respective partners on manganese. The five orbitals, $1a_1$, $2b_2$, $1b_1$, $2a_1$, and $2a_2$, make up the block commonly associated with "ligand field splitting" of the manganese d orbitals. Not surprisingly, the orbital splitting pattern resembles that expected for square-pyramidal coordination of a metal.

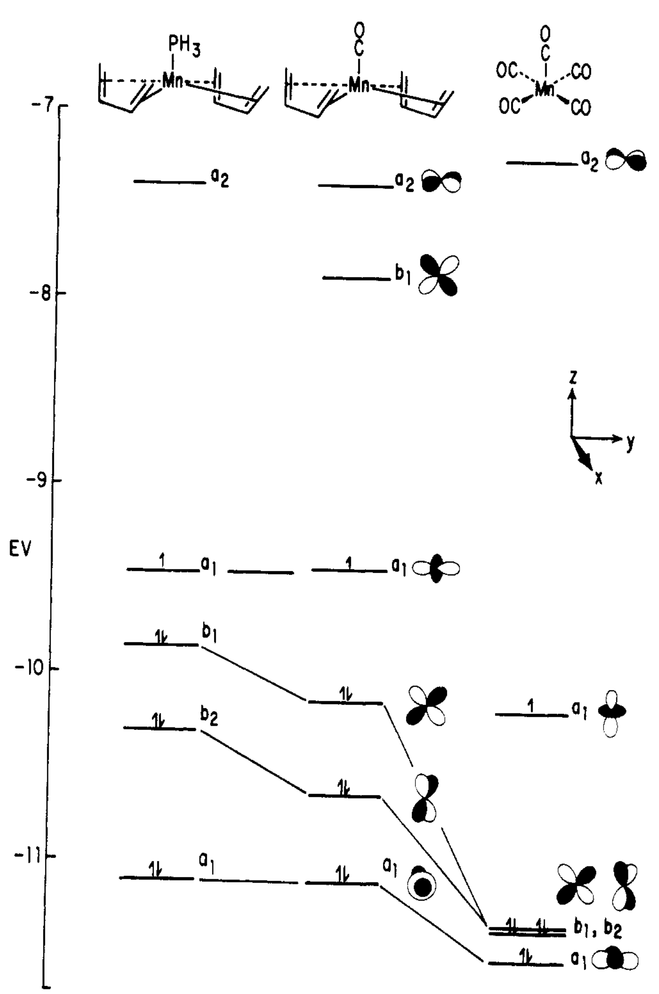

Figure 6. Orbital splitting diagrams for Mn(η-C_4H_6)$_2$L and $Mn(CO)_5$.

Manganese pentacarbonyl, though not isolable under normal conditions, is expected to have C_{4v} symmetry (i.e., a square-pyramidal geometry) based on the theoretical calculations of several groups.[11-14] The orbital splitting diagram has been described previously.[11-13,19] It is compared with that of Mn(C_4H_6)$_2$L (L = PH_3, CO) in Figure 6. First we find that the primary effect of replacing phosphine by carbon monoxide in the butadiene derivative is to lower the b_1 and b_2 orbitals through their ability to retrodatively bond to the carbon monoxide π^* orbitals. (Note also the lowering of a related unfilled b_1 orbital through interaction with the carbon monoxide to become the lowest unoccupied molecular orbital of mainly CO π^* character. The related b_2 orbital remains just above a_2. For $Mn(CO)_5$, both b_1 and b_2 remain slightly above a_2. The exact energetic relationship of unoccupied a_2, b_1, and b_2 is parameter dependent.) However, it does not significantly affect the highest occupied molecular orbital (HOMO) where much of our subsequent discussion will center. Second we find that while energies are different, ordering in the occupied d block orbitals is the same, and, therefore, the singly occupied HOMO is of the same sym-

---

(18) The semiempirical technique used is similar to the extended Hückel technique (Hoffmann, R. *J. Chem. Phys.* **1963**, *39*, 1397. Hoffmann, R.; Lipscomb, W. N. *Ibid.* **1962**, *36*, 2179, 3489; *37*, 2872) but includes a correction for two-body repulsion (Anderson, A. B. *J. Chem. Phys.* **1975**, *62*, 1187). Reference 14 includes the parameter set used except that the manganese orbital energies were as follows: 4s, −9.43; 4p, −5.3; 3d, −10.5 eV.

(19) Hay, P. J. *J. Am. Chem. Soc.* **1978**, *100*, 2411.

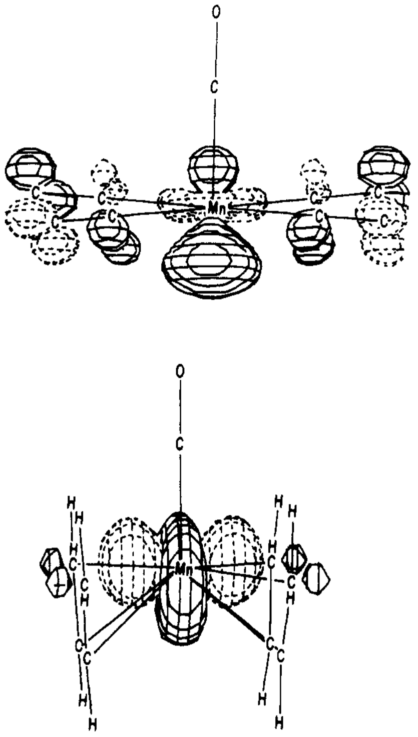

Figure 7. HOMO's of $Mn(CO)_5$ and $Mn(\eta\text{-}C_4H_6)_2(CO)$.

metry in all three cases. However, careful examination of the HOMO wave functions reveals different spatial orientations, and therein, we believe, lies the difference in reactivity of the two species.

A graphical representation of the spatial orientation of the HOMO's of $Mn(CO)_5$ and $Mn(C_4H_6)_2CO$ is shown in Figure 7. Previous analysis[12] has attributed much of the reactivity of $Mn(CO)_5$ to the accessibility of the unpaired electron in a rather unprotected orbital. Furthermore, little or no reorganization of the carbonyl ligands is necessary for dimerization or the interaction with incoming ligands in an associative manner. The latter can readily account for the observed substitutional lability.[2] However, in $Mn(C_4H_6)_2L$ the singly occupied HOMO is not exposed to external attack but rather is "protected" by the atoms of the butadiene groups. More accessibility to the "donut" of this d_{z^2} orbital can be obtained by sliding the butadiene groups up toward the apical ligand, and this does in fact cause a pronounced bulge to appear on the bottom of the "donut". However, the calculated energy to increase the opening by 40° (about what is necessary to permit a phosphite to coordinate) is 50 kcal/mol, which makes it a very unlikely process. Much more ligand reorganization would be required to allow a metal dimer to form, and it is not likely that the energy gained in the formation of a manganese–manganese bond (ca. 35–40 kcal/mol)[20] would offset this energy loss. This description of the HOMO is consistent with the anisotropic ESR parameters observed for these species.

The source of the photochemical substitution lability is not obvious because of the variety of reaction pathways available once the molecule has been energized. However, it is noteworthy that among the lower electronic transitions (Figure 5) the ($a_1 \rightarrow a_2$), ($b_1 \rightarrow b_2$, not shown), and ($b_2 \rightarrow b_1$) transitions are formally forbidden, whereas the ($b_1 \rightarrow a_1$), ($a_1 \rightarrow b_1$), ($a_1 \rightarrow b_2$, not shown), and ($a_1 \rightarrow a_1$) transitions are allowed. Of the allowed transitions, ($a_1 \rightarrow b_1$) and ($a_1 \rightarrow b_2$) will reinforce the Mn–C bond because the electron is removed from a Mn–C nonbonding orbital and placed in an Mn–C π-bonding orbital. On the other hand, the ($1b_1 \rightarrow 2a_1$) transition weakens the Mn–C bond by moving an electron from a π-bonding orbital to a nonbonding orbital. Also, the ($2a_1 \rightarrow 3a_1$) transition weakens the Mn–C bond by moving the electron from a nonbonding to a σ-antibonding orbital.

Acknowledgment. We are grateful for the very capable technical assistance of D. W. Reutter, L. Lardear, and D. Jones. They are deeply indebted to Dr. P. Kasai (IBM Instruments, Inc.) for the computer simulations of the ESR spectra and for his advice concerning the ESR data. P.J.K. thanks Professor P. Rieger for useful discussions.

Registry No. 1, 82963-75-5; 2, 82963-76-6; 3, 82963-77-7; 4, 54688-87-8; 5, 82963-78-8; 6, 82963-79-9; 7, 82963-81-3; 8, 83023-54-5; $MnCl_2$, 7773-01-5; $Mg(C_4H_6)$, 60300-64-3; Mn, 7439-96-5; tetrabutylammonium perchlorate, 1923-70-2; 18-crown-6, 17455-13-9.

Supplementary Material Available: Positional parameters of hydrogen atoms (Table V), thermal parameters (Table VI), least-squares planes (Table VII), and structure factor amplitudes (Table VIII) (19 pages). Ordering information is given on any current masthead page.

---

[20] (a) Haines, L. I. B.; Hopgood, D.; Poë, A. J. *J. Chem. Soc. A* **1968**, 421. (b) Hughey, J. L.; Anderson, C. P.; Meyer, T. J. *J. Organomet. Chem.* **1977**, *125*, C49.